High-Resolution Mapping of Carcinogen Binding Sites on DNA†

T. Christian Boles and Michael E. Hogan*
Department of Molecular Biology, Princeton University, Princeton, New Jersey 08544
Received October 28, 1985; Revised Manuscript Received January 22, 1986

ABSTRACT: We have used a photochemical method to map covalent binding sites of the carcinogen benzo[*a*]pyrenediol epoxide (BPDE) within DNA from the transcriptional control region of the chicken adult β-globin gene. Our preliminary low-resolution mapping has demonstrated that this region contains highly preferred BPDE binding sites [Boles, T. C., & Hogan, M. E. (1984) *Proc. Natl. Acad. Sci. U.S.A. 81*, 5623–5627]. Here, we find that BPDE binding at individual G residues in this region is influenced by nearest-neighbor interactions and also by longer range interactions that may be attributable to sequence-specific variation of DNA secondary structure. Our findings suggest that long poly(dG) sequences should be preferred sites for BPDE action in other genes.

Research over the past 15 years has demonstrated that the carcinogen benzo[*a*]pyrene (BP) is metabolized in eucaryotic cells to a highly reactive electrophile [(+)-*anti*-benzo[*a*]pyrene-7,8-diol 9,10-epoxide] which binds covalently to DNA (Phillips, 1983). That epoxide (BPDE) is believed to be the ultimate carcinogenic form of BP (Newbold & Brooks, 1976; Buenig et al., 1978). The predominant BPDE–DNA adduct results from attack of the N2 position of guanine, comprising 80–90% of all DNA adducts formed in vitro or in vivo (Meehan & Straub, 1979; Jeffrey et al., 1977).

We are interested in the influence of DNA sequence on carcinogen binding and have recently reported a photochemical method which allows us to map covalent BPDE binding sites within cloned eucaryotic DNA fragments (Boles & Hogan, 1984). Our method takes advantage of the fact that BPDE adducts contain an intact pyrene chromophore which absorbs light maximally at 346 nm. We find that when BPDE-modified DNA is irradiated with laser light at 355 nm, single-strand DNA cuts are produced. The photolytic reaction is quantitative; i.e., the cutting probability at each BPDE residue approaches 1 (Boles & Hogan, 1984). We find that the cutting reaction does not depend on diffusible singlet oxygen and that the DNA strand which contains the modified G residue is cleaved specifically, probably due to direct interaction with excited-state pyrene (Boles & Hogan, 1984).

In previous work, we used BPDE-mediated photolysis to map BPDE binding in restriction fragments of the chicken adult β-globin gene (Boles & Hogan, 1984). Following BPDE photolysis, the cleavage products were electrophoresed in denaturing agarose gels. The positions of BPDE binding sites within the gene sequence were then determined from the size of the resulting cleavage products. Our results showed that, at low resolution, BPDE binding within the β-globin gene is distinctly nonrandom. In particular, a 300 base pair (bp) region immediately 5′ to the transcription origin contains a cluster of highly preferred BPDE binding sites (Boles & Hogan, 1984).

Here, we use BPDE-mediated photolysis to examine BPDE binding within that 5′ region of the β-globin gene at single base pair resolution. The goal of this work is to illucidate features of DNA sequence which direct BPDE binding to this globin domain. A longer range goal is to pair these mapping data with data measured in other gene control regions, to produce rules for predicting where BPDE will attack functionally important DNA segments.

Experimental Procedures

BPDE Modification. Supercoiled JW-101 (400 μg/mL) was resuspended in 10 mM tris(hydroxymethyl)aminomethane hydrochloride (Tris-HCl), pH 7.5, 50 mM NaCl, and 10 mM $MgCl_2$ (TMN buffer). A small aliquot of 3 mM (±)-*anti*-[^{3}H]BPDE (403 mCi/mmol) in tetrahydrofuran (THF) was added (final THF concentration 10%). The samples were immediately mixed and transferred to a 37 °C water bath. Reaction mixtures were shielded from light. After 1 h, modified DNA was purified free of noncovalently bound carcinogen by three phenol extractions and ethanol precipitation. DNA concentration was measured by UV absorbance at 258 nm ($\epsilon = 1.3 \times 10^4$ cm^{-1} M^{-1}). Bound carcinogen was determined by liquid scintillation counting. The extent of modification in these experiments was 100 (±20) BPDE adducts per plasmid. BPDE was obtained from the Midwest Research Institute.

End Labeling. For details of the construction of JW-101 and a diagram of pertinent restriction sites, see Figure 1.

To examine the BPDE binding sites on the strand corresponding to that which acts as the template for mRNA transcription, modified pJW-101 was first cleaved with *Hin*dIII. The DNA was then 3′ end labeled with the Klenow fragment of DNA polymerase I and [α-^{32}P]dNTP's (Maniatis et al., 1982). DNA was purified by phenol extraction and ethanol precipitation. Secondary cleavage was performed with *Hpa*II. The 600 bp *Hin*dIII–*Hpa*II fragment was purified by acrylamide gel electrophoresis (Maxam & Gilbert, 1980) to yield a fragment which is singly end labeled at the 3′ terminus of the *Hin*dIII site. To examine BPDE binding sites on the strand complementary to the template strand, BPDE-modified plasmid was cleaved with *Sau*3A and 3′ end labeled with Klenow fragment. After phenol extraction and ethanol precipitation, a 400 bp *Sau*3A fragment was purified from gels as above. Secondary cleavage was performed with *Hin*dIII, and the 93 bp *Sau*3A–*Hin*dIII fragment was purified from a second preparative gel. This fragment contains label only at the 3′ terminus of the *Sau*3A site. All enzymes were obtained from Boehringer Mannheim. Nucleotides were obtained from New England Nuclear.

BPDE Photolysis. End-labeled restriction fragments were irradiated for 5 min at 20–30-mW continuous power with 355-nm laser light (the frequency-tripled output of the Mo-

† This work is supported by a grant from the National Cancer Institute.

0006-2960/86/0425-3039$01.50/0

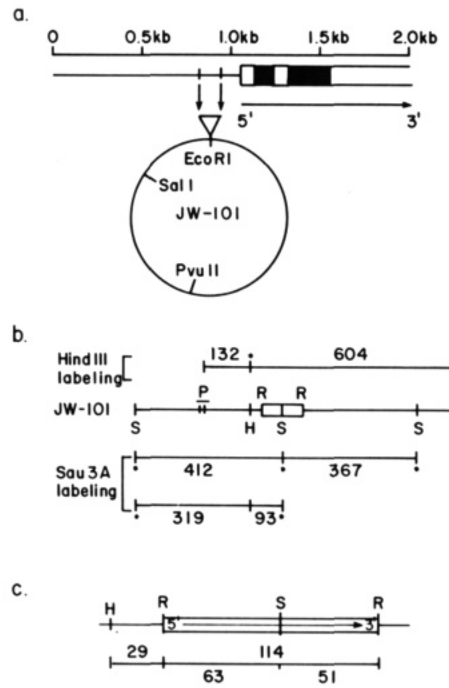

FIGURE 1: (a) Construction of JW-101. The 5′ half of the chicken adult β-globin gene is shown at the top of the figure. The thickened region indicates the mRNA transcription unit. Shaded areas are the coding regions of the gene. The 114 base pair (bp) *Msp*I fragment extending from −225 to −111 bp (with respect to the origin of transcription) is indicated by the hash marks in the 5′ flanking region. This fragment was inserted into the *Eco*RI site of pBR322 to form JW-101 (Wang & Hogan, 1985). (b) End labeling. This shows the restriction sites which were used for end labeling. The center of the figure shows an expanded restriction map of JW-101 in the immediate vicinity of the insert. Restriction sites for *Eco*RI (R), *Hin*dIII (H), *Sau*3A (S), and *Hpa*II (P) are shown. The upper and lower portions of the figure show the labeled fragments that are generated during the *Hin*dIII and *Sau*3A labeling protocols, respectively. The 3′ end labeled termini are indicated by asterisks. Lengths of the fragments are given in base pairs (bp). (c) Detailed structure of the insert. This shows a further expansion of the JW-101 insert region. Also shown is the orientation of the insert DNA within the plasmid with respect to its orientation in the chicken adult β-globin gene. Restriction sites are symbolized as in Figure 1b.

lectron MY-30 laser) as described (Boles & Hogan, 1984).

Results and Discussion

BPDE-Mediated Photolysis. The construction of the plasmid pJW-101 has been described (Wang & Hogan, 1985). This plasmid contains the chicken globin gene sequence from −225 to −111 (with respect to the origin of transcription) inserted into the *Eco*RI site of pBR322. A schematic diagram of the plasmid and the location of the insert sequence in the chicken gene are presented in Figure 1a.

Supercoiled pJW-101 was modified with BPDE to 100 (±20) covalent adducts per plasmid (1 per 96 bases). Insert-containing restriction fragments of BPDE-modified plasmids were singly end labeled with Klenow fragment and [α-^{32}P]dNTP's. For a detailed description of fragment preparation, see Experimental Procedures.

DNA fragments were then irradiated with 355-nm laser light and electrophoresed with appropriate unirradiated controls in 8% acrylamide–8 M urea sequencing gels. An autoradiogram of such a gel is shown in Figure 2.

Our previous work suggested that BPDE-mediated photolysis is localized to the nucleotide residue to which it is bound (Boles & Hogan, 1984). High-resolution gel analysis of BPDE cleavage sites can confirm such a mechanism unambiguously. For example, if the photochemically activated pyrene moiety

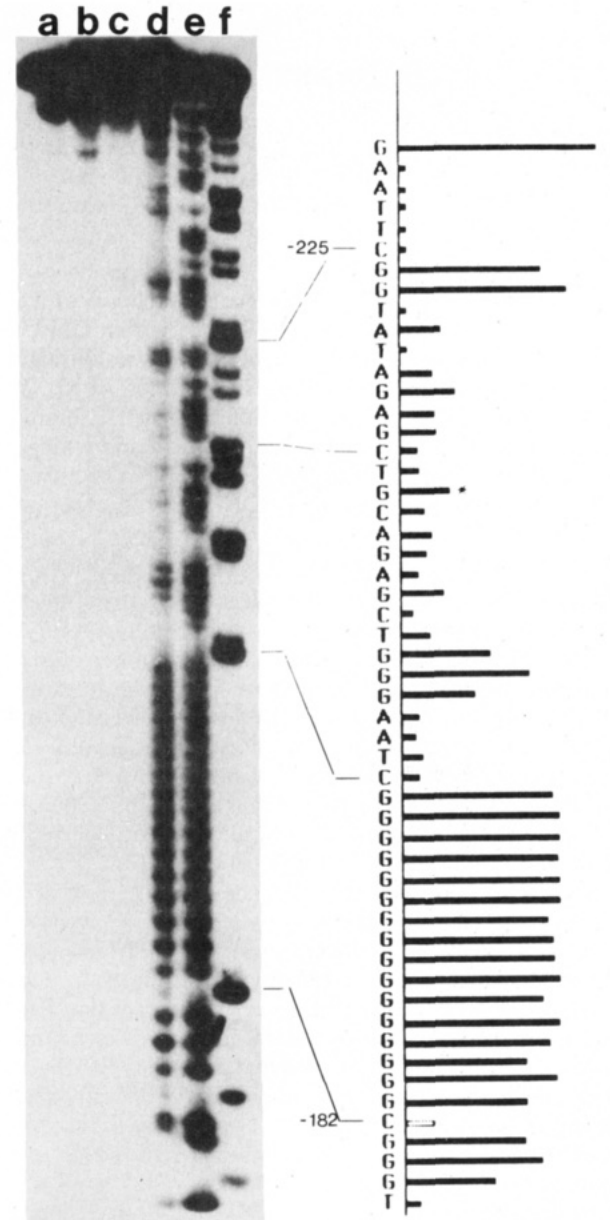

FIGURE 2: High-resolution mapping of BPDE binding sites. The 93 bp *Hin*dIII–*Sau*3A fragment from JW-101 was 3′ end labeled at the *Sau*3A site as detailed in Figure 1b. DNA samples were irradiated for 5 min at 20–30-mW continuous power with 355-nm laser light and electrophoresed in an 8% denaturing acrylamide gel (Maxam & Gilbert, 1980). Lanes a, b, e, and f are unmodified DNA samples. Lanes c and d are BPDE-modified samples. Lanes b and d were irradiated with 355-nm laser light. Lanes a and c are unirradiated control samples. Lanes e and f are G + A and C + T Maxam and Gilbert sequencing ladders, respectively (Maxam & Gilbert, 1980). The right portion of the figure shows the BPDE cutting (binding) intensity at each position of the sequence as determined from a densitometric tracing of lane d, superimposed upon the base sequence of this region. Numbers to the left of the sequence signify position relative to the β-globin transcription origin.

cuts DNA at the G residue to which it is covalently attached, then the cleavage product might be expected to comigrate with the corresponding fragment produced by a Maxam and Gilbert G-specific cleavage reaction, depending on the detailed structure of the cleaved end (presence of BPDE photoproduct, presence of 5′-phosphate on terminal residue, etc.). The set of cleavage products might therefore resemble a G ladder. On the other hand, if activated pyrene attacks nucleotide residues immediately adjacent to the modified G residue, then a +1 or −1 base G ladder might be generated.

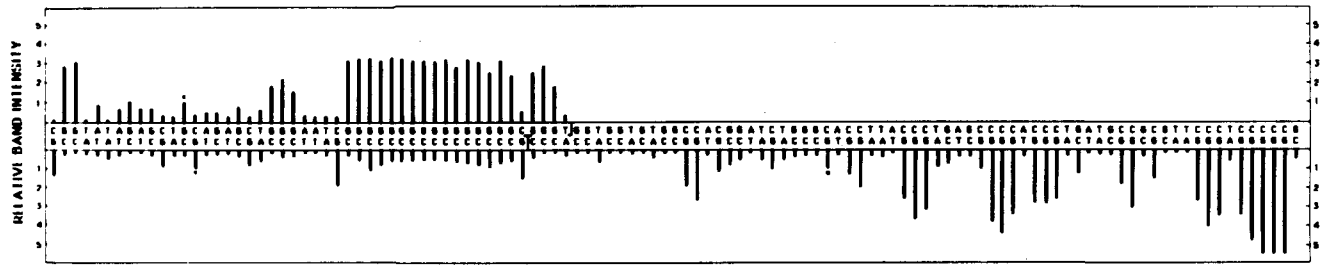

FIGURE 3: Summary of BPDE binding sites within the JW-101 insert. The data of three mapping experiments as shown in Figure 2 are compiled in this figure. The numbering of the sequence is from left to right, −225 to −111 relative to the globin transcription origin; i.e., the right side of this figure represents the sequence that is proximmal to the mRNA start site. The upper portion of the figure displays the BPDE cutting distribution for the nontemplate strand as mapped by 3′ end labeling of the *Sau*3A site (BPDE binding in the region from −177 to −111 of the nontemplate strand has not been examined). The lower portion of the figure displays the data for the template strand (obtained from two gels not shown) mapped by 3′ end labeling of the *Hin*dIII site. The boundaries of data from each mapping experiment are marked by small brackets. Cutting probability at each position of the sequence was obtained from densitometric tracings of the autoradiograms. Asterisks mark reference G residues which were defined to have a value of 1 in the calculation of relative binding affinity (see text for details).

The data of Figure 2 demonstrate that the G-specific cleavage products produced by our assay comigrate with the G-specific products produced by a standard Maxam and Gilbert G + A cleavage reaction. This constitutes good evidence that photochemical cleavage induced by our method occurs at the G residue which is covalently modified by the carcinogen.

Since sequencing gel systems are designed to resolve molecules that differ by very small increments of charge and molecular weight, comigration of products is consistent with the idea that they have identical phosphate termini. The Maxam and Gilbert protocols are known to cause a β-elimination of the 3′-phosphate group, cleaving the DNA backbone between C3′ and O3′ (Maxam and Gilbert, 1980). The DNA fragment 3′ to the cleavage site is left with a 5′-phosphate terminus (Maxam & Gilbert, 1980). Therefore, by analogy, it appears that BPDE photolysis also involves cleavage of the DNA between C3′ and O3′ of the modified guanine nucleotide. Work is in progress to define the nature of these termini, biochemically.

BPDE Binding at G, A, and C. We have determined the extent of BPDE-mediated cleavage at each position in the sequence from densitometric scans of the autoradiograms. The result of these analyses is shown in Figure 3. We have expressed the amount of cutting at each position as the ratio of optical density associated with a particular band to that of a reference cutting site in the sequence. The reference position for each gel was chosen to be the G in the sequence $^{5'}$TGC$^{3'}$. This normalized quantity should be proportional to the likelihood of BPDE-mediated cutting at each position in the sequence. In earlier work, we have shown that BPDE-mediated DNA cutting is quantitative under our assay conditions (Boles & Hogan, 1984). Therefore, at the covalent binding density we have employed (1 BPDE per 96 bases), the likelihood of multiple photochemical cuts within the regions we have mapped is small. We have confirmed that the data of Figure 3 correspond to single-hit statistics by repeating the measurements at 1 BPDE per 200 bases (not shown). Because the data have been measured at a low cut density, the distribution of BPDE-mediated cuts in this assay is therefore equivalent to the distribution of bound molecules.

The data summarized in Figure 3 show that BPDE-mediated photolysis occurs primiarly at G residues. This is consistent with the fact that the major BPDE adduct occurs at guanine (Meehan & Straub, 1979; Jeffrey et al., 1977).

We have not detected any specific BPDE cleavage products at T residues. However, we do detect products which appear to result from cleavage at a few A (see the left end of the nontemplate strand in Figure 3) and C residues [see the 15-base poly(C) tract of the template strand, and other positions scattered throughout the sequence]. Cutting probability at these few positions is always low but appears to be above background. These findings are consistent with the known base specificity of BPDE binding: adenine and cytosine may comprise 5–10% of all covalent adducts formed in vitro (Meehan & Straub, 1979).

Table I: Nearest-Neighbor Analysis of BPDE Binding Sites[a]

3′ base	base 5′ to BPDE binding site: G	A	T	C
G	3.40 ± 0.82 (24)	2.75 ± 0.66 (4)	2.62 ± 0.82 (3)	3.39 ± 1.15 (5)
A	2.50 ± 0.95 (3)	0.87 ± 0.32 (3)	no data	1.90 (1)
T	2.30 ± 0.74 (5)	no data	no data	1.10 (1)
C	1.77 ± 0.58 (4)	0.77 ± 0.05 (4)	1.00 ± 0.00 (3)	1.50 ± 0.00 (2)

[a] The data of Figure 3 were analyzed to show the effect of 3′ and 5′ nearest neighbors on the BPDE binding probability. Each G in the sequence was classified according to its nearest neighbors. The relative binding (cutting) probability at the central G in each triplet class was calculated. Also shown is the standard deviation of the data. The number of observations of each triplet type is shown in parentheses. To illustrate, the average probability of BPDE binding to the central G residue in the three $^{5'}$GGA$^{3'}$ triplets is 2.50 ± 0.95 relative to an isolated G.

It is likely that the structure of the A and C adduct differs substantially from that with G residues. It is therefore interesting that these adducts appear to be cleaved in our photochemical assay. Unfortunately, since these secondary adducts comprise such a small fraction of the total, we cannot quantify the cutting efficiency at these positions. In the absence of such quantification, which is now in progress using synthetic helices, the measured distribution of BPDE-mediated cuts at A and C cannot be related to the binding distribution in a simple way.

Nearest-Neighbor Effects on BPDE Binding Residues. One important conclusion that can be drawn from the data of Figure 3 is that the likelihood of BPDE binding to individual G residues is not constant but varies throughout the sequence. The range of relative values is from 1 to approximately 5 in this DNA sequence. To examine possible origins of this heterogeneity, we have analyzed the influence of nearest-neighbor interactions on BPDE binding to G. Each G in the sequence was classified according to its 5′ and 3′ neighbors. The relative probability of binding to the central G residue in each of the 16 possible $^{5'}$XGX$^{3'}$ triplet classes was cataloged from the data displayed in Figure 3 and then averaged. Those values and their standard deviations are displayed in Table I.

The most obvious effect seen in Table I is that of neighboring G residues. The central G of the sequence $^{5'}XGG^{3'}$ (where X is any of the four bases) has an intrinsic BPDE binding probability that is 2.6–3.4-fold greater than that of the reference sequence $^{5'}TGC^{3'}$. Similarly, the central G of the sequence $^{5'}GGX^{3'}$ shows binding that is 1.8–3.4 times that of the reference level. Evidently, G nearest neighbors increase the probability of BPDE binding substantially.

Other nearest-neighbor interactions do not seem to influence BPDE binding. Although the number of observations is too small to be analyzed quantitatively, $^{5'}XGX^{3'}$ sequences, where X is not G, seem to display a binding probability that approaches the reference value (Table I).

Further analysis of the data of Figure 3 and Table I suggests that the effect of nearest neighbors may be directional. For example, in Figure 3, the G on the 3′ end of a run of two or more G residues shows a lower cutting (binding) probability than its immediate 5′ neighbor. In contrast, the G residue on the 5′ end of poly(G) tracts always displays a binding probability which is greater than or nearly equal to its 3′ neighbor. The trend can also be seen in the data of Table I.

As discussed above, the effect of having a G as a 5′ nearest neighbor also increases the BPDE binding probability at G. Intercalating dyes are known to cause structural perturbations that affect base pairs on either side of the binding site (Breloff & Crothers, 1975). In previous work, we have demonstrated that BPDE binding affects a local domain in at least 4 bp and induces a large (approximately 30°) bend in the axis of the helix (Hogan et al., 1981). It therefore seems possible that sequences to either side of an intercalated BPDE complex can influence binding by allowing, or alternatively by inhibiting, BPDE-induced distortion in the regions surrounding the binding site.

We emphasize that the effect of G nearest neighbors should not be interpreted as the result of interactions between BPDE adducts. The experiments presented in Figures 2 and 3 were carried out with DNA samples that contained an average of 1 adduct per 50 bp. The probability of binding at two adjacent G residues in a given 50 bp sequence is therefore very small. In addition, we have repeated some of the experiments with DNA samples which were modified to an average of 1 adduct per 100 base pairs with identical results (data not shown). Therefore, we are confident that our results are free from artifacts arising from interactions between closely spaced carcinogen molecules.

Enhanced BPDE Binding at Poly(G) Tracts. The influence of G nearest neighbors on BPDE binding may extend beyond nearest-neighbor interactions. From the data in Figure 3, there appears to be a correlation between the size of a poly(G) tract and the average likelihood of BPDE binding within a tract. To examine this phenomenon, we have classified each G in the globin sequence according to the size of the poly(G) tract in which it occurs, and we have averaged BPDE binding values for each poly(G) size class. The data are shown in Figure 4.

Taken at face value, the data suggest that the likelihood of BPDE binding within a poly(G) tract may pass through a maximum as tract length increases from 4 to 16 bp. However, this result must be interpreted with caution since there are few occurrences of poly(G) tracts longer than 3 bp in the sequence analyzed. Until additional data are obtained, we prefer the more conservative interpretation that the probability of BPDE binding appears to reach a maximum value at poly(G) tract lengths around 4–5 bp long. BPDE binding probability at the plateau is probably in the range of 3–4, relative to an isolated G.

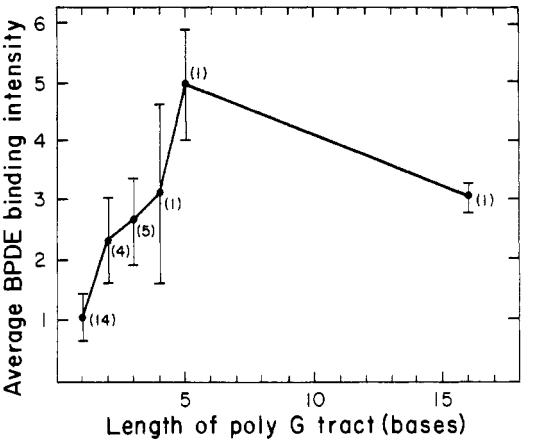

FIGURE 4: BPDE binding affinity in poly(dG) tracts. The data of Figure 3 were analyzed. BPDE binding probability was analyzed at G residues in sequences of the form $^{5'}N(G)_nN^{3'}$ [where N is not G and *n* signifies the number of consecutive G residues in a poly(G) tract]. Average binding probability to individual G residues in each poly(G) class is shown as a function of the poly(G) tract length *n*. The error bars indicate 1 standard deviation of the data. The numbers in parentheses indicate the number of poly(G) tracts analyzed. For example, there were five instances of the sequence $^{5'}NGGGN^{3'}$; the value shown is therefore the average of 15 individual BPDE binding values. In those instances where a sequence appears only once, error bars refer to the distribution of cutting probability at G sites within that segment only.

Such behavior could be interpreted as an indication that the carcinogen is actually in contact with 4–5 consecutive base pairs at its binding site. However, that interpretation is unlikely because the dimensions of the BPDE molecule make it impossible for the carcinogen to span more than 3 bp. Also, other lines of evidence suggest that BPDE forms a two base pair long intercalated complex (Hogan et al., 1981; Drinkwater et al., 1978).

Alternatively, it is possible that a poly(G) sequence can assume a local secondary structure which favors BPDE binding. It has been known for some time that the helix poly(dG)·poly(dC) displays circular dichroism which is different from that of its sequence isomer (Wells et al., 1970). X-ray diffraction data on poly(dG)·poly(dC) sequences have been interpreted as suggesting that such helices prefer an A-like rather than the traditional B DNA helix geometry (Arnott & Selsing, 1974; Wang et al., 1982). Recent studies on the sequence specificity of DNA cutting by DNase II and the phenanthroline–Cu^{2+} complex are also consistent with the idea that poly(dG)·poly(dC) sequences adopt an A-like conformation in solution (Drew & Travers, 1983).

It is interesting to consider the properties of A DNA in light of our results and an intercalative model for BPDE binding. Of particular interest are the features of the minor groove. In A DNA, the minor groove is very wide and shallow compared to a B DNA helix (Dickerson et al., 1982). Guanine nitrogen N2 (the preferred BPDE binding site) faces outward into the small groove. If poly(dG)·poly(dC) segments are predisposed to assume an altered A-like geometry, guanine N2 may be more accessible to attack in that conformation.

The DNA region we have mapped at one-base resolution is interesting in structural terms, because it has been shown to possess a DNA segment (the sequence G_{16}, 27 nucleotides from its 5′ end) which can assume a distorted, S1 nuclease sensitive conformation in supercoiled plasmid molecules (Wang & Hogan, 1985; Schon et al., 1983; Nickol & Felsenfeld, 1983).

Since the mapping experiments described here were performed on a supercoiled DNA substrate, it is possible that the

conformational equilibrium which exists at the poly(G) site could contribute to the distribution of bound BPDE molecules which we have mapped there (Figure 3). As we discuss elsewhere (Wang & Hogan, 1985), the equilibrium between the distorted and undistorted conformations is such that less than 10% of plasmid molecules display the distorted conformation in the reaction buffers we employ.

In work which we present elsewhere (Boles & Hogan, 1985), we use indirect enzymatic methods to show that BPDE does indeed bind preferentially to the distorted poly(G) conformer. However, because that site constitutes a minority component of the equilibrium, specific binding to the S1-sensitive conformation at G_{16} is averaged in with binding to the (predominant) S1-insensitive species in the direct photochemical mapping experiments presented here. Work is now in progress in our laboratory to enhance the fraction of poly(G) segments in that distorted state so that BPDE binding to that rare structure may be studied directly. For now, it is interesting to note that there is increased cutting at C within the region (Figure 3). It is possible that this effect could be a manifestation of BPDE binding to the rare conformer at this site.

Conclusions

We have shown that the likelihood of BPDE binding to individual G residues is affected by the surrounding sequence and can be enhanced 3–4-fold in certain contexts (Figure 3). Nearest-neighbor analysis suggests that the BPDE binding may be asymmetric, with a significant preference for a G nearest neighbor on the 3′ side (Table I).

We have observed enhanced BPDE binding within poly(G) tracts. In poly(G) tracts that are greater than or equal to 4 bp long, each individual G residue displays a BPDE binding affinity which is at least 3-fold greater than that with non-G nearest neighbors (Figure 4). We suggest that poly(dG)·poly(dC) DNA possesses a secondary structure conducive to BPDE binding. It is possible that part of this effect is related to the fact that poly(dG)·poly(dC) tracts adopt an A-like conformation in solution, thus facilitating BPDE binding from the minor groove side of the helix. We believe that the ability of poly(dG)·poly(dC) to accommodate BPDE-induced distortion in the regions surrounding the binding site during covalent modification might also contribute to the measured binding preference.

Our data also suggest that the biological effects associated with BPDE binding may be preferentially targeted to chromosomal regions that are rich in poly(G) sequences. Work is in progress to test that concept.

Acknowledgments

We thank Robert Austin for the use of the Nd-YAG laser.

Registry No. BPDE, 63323-31-9.

References

Arnott, S., & Selsing, E. (1974) *J. Mol. Biol. 88*, 551–552.

Boles, T. C., & Hogan, M. E. (1984) *Proc. Natl. Acad. Sci. U.S.A. 81*, 5623–5627.

Boles, T. C., & Hogan, M. E. (1985) *Biochemistry* (submitted for publication).

Bresloff, J. L., & Crothers, D. M. (1975) *J. Mol. Biol. 95*, 103–123.

Buening, M. K., Wislocki, P. G., Levin, W., Yagi, H., Thakker, D. R., Akagi, H., Koreeda, M., Jerina, D. M., & Conney, A. H. (1978) *Proc. Natl. Acad. Sci. U.S.A. 75*, 5358–5361.

Dickerson, R. E., Drew, H. R., Conner, B. N., Wing, R. M., Fratini, A. Y., & Kopka, M. L. (1982) *Science (Washington, D.C.) 216*, 475–485.

Drew, H. R., & Travers, A. A. (1983) *Cell (Cambridge, Mass.) 37*, 491–502.

Drinkwater, N., Miller, J. A., Miller, E. C., & Yang, N. C. (1978) *Cancer Res. 38*, 3247–3255.

Hogan, M. E., Dattagupta, N., & Whitlock, J. P. (1981) *J. Biol. Chem. 256*, 4504–4513.

Jeffrey, A. M., Weinstein, I. B., Jennette, K. W., Grzeskowiak, K., Nakanishi, K., Harvey, R. G., Autrup, H., & Harris, C. (1977) *Nature (London) 269*, 348–350.

Maniatis, T., Fritsch, E. B., & Sambrook, J. (1982) *Molecular Cloning: A Laboratory Manual*, pp 113–121, Cold Spring Harbor Laboratory, Cold Spring Harbor, NY.

Maxam, A., & Gilbert, W. (1980) *Methods Enzymol. 65*, 497–559.

Meehan, T., & Straub, K. (1979) *Nature (London) 277*, 410–412.

Newbold, R. F., & Brookes, P. (1976) *Nature (London) 261*, 52–54.

Nickol, J. M., & Felsenfeld, G. (1983) *Cell (Cambridge, Mass.) 35*, 467–477.

Phillips, D. H. (1983) *Nature (London) 303*, 468–472.

Schon, E., Evans, T., Welsch, J., & Efstratiadis, A. (1983) *Cell (Cambridge, Mass.) 35*, 837–848.

Wang, A. H.-J., Fujii, S., van Bloom, J. H., & Rich, A. (1982) *Proc. Natl. Acad. Sci. U.S.A. 79*, 3968–3972.

Wang, J. C., & Hogan, M. (1985) *J. Biol. Chem. 260*, 8194–8202.

Wells, R. D., Larson, J. E., Grant, R. C., Shortle, B. E., & Cantor, C. R. (1970) *J. Mol. Biol. 54*, 465–497.